Neurobiology of Disease 153 (2021) 105332

Contents lists available at ScienceDirect

Neurobiology of Disease

journal homepage: www.elsevier.com/locate/ynbdi

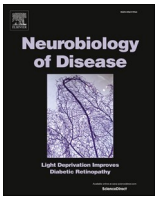

Dermal and cardiac autonomic fiber involvement in Parkinson's disease and multiple system atrophy

Joachim Brumberg [a,*], Anastasia Kuzkina [b], Constantin Lapa [a,c], Sona Mammadova [b], Andreas Buck [a], Jens Volkmann [b], Claudia Sommer [b], Ioannis U. Isaias [b], Kathrin Doppler [b]

[a] Department of Nuclear Medicine, University Hospital Würzburg and Julius-Maximilian-University Würzburg, Oberdürrbacher Straße 6, 97080 Würzburg, Germany
[b] Department of Neurology, University Hospital Würzburg and Julius-Maximilian-University Würzburg, Josef-Schneider-Straße 11, 97080 Würzburg, Germany
[c] Nuclear Medicine, Medical Faculty, University of Augsburg, Stenglinstraße 2, 86156 Augsburg, Germany

ARTICLE INFO

J. Timothy Greenamyre

Keywords:
Peripheral nervous system
Parkinson's disease
Skin biopsy
MIBG scintigraphy
Multiple system atrophy

ABSTRACT

Pathological aggregates of alpha-synuclein in peripheral dermal nerve fibers can be detected in patients with idiopathic Parkinson's disease and multiple system atrophy. This study combines skin biopsy staining for p-alpha-synuclein depositions and radionuclide imaging of the heart with [^{123}I]-metaiodobenzylguanidine to explore peripheral denervation in both diseases. To this purpose, 42 patients with a clinical diagnosis of Parkinson's disease or multiple system atrophy were enrolled. All patients underwent a standardized clinical work-up including neurological evaluation, neurography, and blood samples. Skin biopsies were obtained from the distal and proximal leg, back, and neck for immunofluorescence double labeling with anti-p-alpha-synuclein and anti-PGP9.5. All patients underwent myocardial [^{123}I]-metaiodobenzylguanidine scintigraphy. Dermal p-alpha-synuclein was observed in 47.6% of Parkinson's disease patients and was mainly found in autonomic structures. 81.0% of multiple system atrophy patients had deposits with most of cases in somatosensory fibers. The [^{123}I]-metaiodobenzylguanidine heart-to-mediastinum ratio was lower in Parkinson's disease than in multiple system atrophy patients (1.94 ± 0.63 vs. 2.91 ± 0.96; $p < 0.0001$). Irrespective of the diagnosis, uptake was lower in patients with than without p-alpha-synuclein in autonomic structures (1.42 ± 0.51 vs. 2.74 ± 0.83; $p < 0.0001$). Rare cases of Parkinson's disease with p-alpha-synuclein in somatosensory fibers and multiple system atrophy patients with deposits in autonomic structures or both fiber types presented with clinically overlapping features. In conclusion, this study suggests that alpha-synuclein contributes to peripheral neurodegeneration and mediates the impairment of cardiac sympathetic neurons in patients with synucleinopathies. Furthermore, it indicates that Parkinson's disease and multiple system atrophy share pathophysiologic mechanisms of peripheral nervous system dysfunction with a clinical overlap.

1. Introduction

Deposition of alpha-synuclein aggregates in neurons and glia can be found in idiopathic Parkinson's disease (PD) and multiple system atrophy (MSA) (Dickson et al., 1999; Dickson et al., 2009). Its accumulation is supposed to play a key role in the pathophysiology of both diseases, but underlying mechanisms by which alpha-synuclein contributes to cellular dysfunction and neuronal cell loss and its pathophysiologic spread throughout the nervous system are still not fully understood (Borghammer, 2018; Burre et al., 2018; Rocha et al., 2018). In PD, alpha-synuclein aggregates are typically found in neurons forming so-called Lewy bodies, whereas in MSA oligodendrocytes are predominantly affected by glial cytoplasmic inclusions (Dickson et al., 1999; Dickson et al., 2009; Spillantini, 1999).

The in vivo demonstration of phosphorylated alpha-synuclein (p-alpha-syn) deposits within neurons and neurites outside the central nervous system is a recent advancement for histopathological confirmation of PD (Donadio et al., 2014; Doppler et al., 2014; Lebouvier

Abbreviations: PD, Parkinson's disease; MSA, multiple system atrophy; p-alpha-syn, phosphorylated alpha-synuclein; MIBG, [^{123}I]-metaiodobenzylguanidine; SNAP, sensory nerve action potential; IENFD, intraepidermal nerve fiber density; TH, tyrosine hydroxylase; VIP, vasoactive intestinal peptide; ROI, region-of-interests; HM, heart-to-mediastinum..

* Corresponding author at: Oberdürrbacher Straße 6, 97080 Würzburg, Germany.
E-mail address: Brumberg_J@ukw.de (J. Brumberg).

https://doi.org/10.1016/j.nbd.2021.105332
Received 11 December 2020; Received in revised form 17 February 2021; Accepted 9 March 2021
Available online 17 March 2021

et al., 2010; Vilas et al., 2016). Histological specimens of skin are particularly easy to obtain, and p-alpha-syn immunoreactivity in dermal nerve structures may allow differentiation of PD from tauopathies and other forms of parkinsonism (Donadio et al., 2014; Doppler et al., 2014; Doppler et al., 2015). Patients with MSA also show p-alpha-syn-positive dermal nerve fibers but affected fiber types differ from PD: in MSA, depositions have mainly been observed in somatosensory fibers of the subepidermal plexus, while they predominantly occur in autonomic dermal nerve fibers in PD (Donadio et al., 2018b; Doppler et al., 2015). Similarly, differences between the two disorders are known from cardiac [^{123}I]-metaiodobenzylguanidine (MIBG) uptake, which is a measure of the integrity of postganglionic, presynaptic sympathetic nerve terminals of the heart (Orimo et al., 1999). MIBG uptake is typically clearly reduced in PD, but not or only slightly reduced in patients with MSA (Orimo et al., 2012; Treglia et al., 2012).

Our study explores the association of dermal p-alpha-syn depositions, dermal autonomic denervation, and cardiac denervation in PD and MSA patients to disentangle the role of alpha-synuclein in peripheral neurodegeneration and to evaluate the diagnostic yield of both methods.

2. Material and methods

2.1. Patients

All patients were in- or outpatients at the Department of Neurology, University Hospital Würzburg, Würzburg, Germany. Thirty-seven patients were prospectively enrolled between August 2017 and December 2018. Data for an additional nine patients originated from prior studies examining p-alpha-syn depositions in skin biopsies (Doppler et al., 2014; Doppler et al., 2015). All 46 participating subjects underwent a standardized clinical work-up including neurological examination, nerve conduction studies, and blood samples for detection of levels of vitamins B12 and B6, methyl malonic acid, and HbA1c. Patients with reduced sensory nerve action potential (SNAP) or nerve conduction velocity were excluded from assessment of dermal innervation. Hypovitaminoses and diabetes mellitus were excluded as potential competing causes of peripheral nerve impairment. Diagnosis was based on current guideline criteria for PD (Postuma et al., 2015) and MSA (Gilman et al., 2008) blinded to MIBG scintigraphy results. To additionally assess the strength of clinical diagnoses and to identify patients with overlapping features of MSA and PD, we evaluated the following criteria for each patient: disease progression (disease duration (years)/H&Y stage < 2: MSA; > 2: PD), autonomic dysfunction (severe: MSA; minor/none: PD), response to levodopa (poor: MSA; good: PD), and, if available, [^{18}F]fluorodeoxyglucose positron emission tomography (hypometabolism of the [posterior] putamen and the cerebellum: MSA; hypermetabolism of the striatum or normal striatal uptake: PD) and magnetic resonance imaging (putaminal or infratentorial atrophy: MSA; not present: PD) (Krismer et al., 2019; Meyer et al., 2017). The number of features for MSA and PD were added and resulted in a score for each disease. If the scores differed by two or more, the patients were assumed to have PD or MSA with typical clinical presentation (tPD, tMSA). In cases where the scores differed by less than two, the symptoms were considered as "overlapping", indicating atypical PD or atypical MSA (PD/MSA overlap).

2.2. Skin biopsy

5-mm skin punch biopsies were obtained from the distal and proximal leg, back (Th10), and neck (C7) under local anesthesia and cryopreserved at −80 °C. 20 μm serial sections were cut as previously described (Doppler et al., 2017). Three consecutive 40-μm sections were separately cut for assessment of intraepidermal nerve fiber density (IENFD).

2.3. Immunofluorescence labeling

Double immunofluorescence labeling with mouse anti-p-alpha-syn (Biolegend, San Diego, California, USA; 1:500) and rabbit anti-PGP9.5 (Zytomed Systems, Berlin, Germany; 1:200), rabbit anti-tyrosine hydroxylase (TH, Synaptic Systems, Göttingen, Germany; 1:500), or rabbit anti-vasoactive intestinal peptide (VIP, Immunostar, Hudson, USA; 1:1000), and appropriate secondary antibodies (Dianova, Hamburg, Germany) was performed as previously described (Doppler et al., 2014). Single immunofluorescence labeling of 40-μm sections with anti-PGP9.5 was done for assessment of IENFD.

2.4. Microscopy

IENFD was assessed according to published counting rules (Lauria et al., 2005) using a fluorescence microscope (Axiophot 2, Zeiss, Oberkochen, Germany) with an Axiocam MRm camera (Zeiss) and SPOT software (Diagnostic Instruments, Sterling Heights, Michigan, USA). All other slides were evaluated using a fluorescence microscope (Ax10, Zeiss) with CARVII system and Visiview software (Visitron GmbH, Puchheim, Germany). Innervation of erector pili muscles was quantified by taking z stacks (0.5 μm distance). A straight line was drawn perpendicularly to the pilomotor nerve fibers at three levels of the muscle, crossing nerve fibers per μm were counted, and the mean value calculated using ImageJ (National Institutes of Health, Bethesda, Maryland, USA) (Schneider et al., 2012). Sweat gland innervation was quantified by taking z stacks (0.5 μm distance), obtaining maximum projections and calculating the percentage of immunolabeled area per sweat gland area using Image J. Due to high background staining and autofluorescence of sweat gland vesicles, a different method was applied for the quantification of noradrenergic and cholinergic sudomotor innervation: the ratio of tubuli per sweat gland, of which the circumference was at least 50%, surrounded by anti-TH−/anti-VIP-immunoreactive fibers was calculated. Skin biopsies were classified as p-alpha-syn-positive if at least one nerve fiber was p-alpha-syn-immunoreactive. For quantification, the ratio of positive biopsy sites per patient (i.e., positive biopsy sites/total number of biopsy sites), the number of p-alpha-syn-positive structures, and the ratio of p-alpha-syn-positive structures divided through the total number of autonomic structures per biopsy was calculated. For quantification of p-alpha-syn in anti-TH- and anti-VIP-positive fibers, the biopsies with p-alpha-syn within anti-TH−/anti-VIP-positive fibers was determined.

2.5. Nerve conduction studies

Neurography of the sural nerve was performed using surface electrodes following standard procedures (Kimura, 2013), and was assessed based on our normal laboratory values (SNAP $\geq$ 10 μV for age $<$ 65 years, amplitude $\geq$ 5 μV for age $\geq$ 65 years, nerve conduction velocity $>$ 40 m/s for all ages).

2.6. MIBG scintigraphy

Imaging was performed within 30 days after skin biopsy in 77.2% of the patients (median 2.5 (range 0–677) d). Medication with known interference with MIBG uptake was discontinued prior to imaging as recommended by current guidelines (Bombardieri et al., 2010; Flotats et al., 2010). MIBG studies were acquired on a dual-headed SPECT/CT system (Symbia T2, Siemens Healthineers, Erlangen, Germany), equipped with a medium-energy, low-penetration collimator. Anterior and posterior planar images were obtained 240 min after the injection of 179.5 ± 6.6 MBq MIBG. MIBG uptake was semi-quantitatively assessed using the PMOD image analysis software version 3.7 (PMOD Technologies Ltd., Zurich, Switzerland). First, three experienced nuclear medicine physicians blinded to the clinical information independently defined region-of-interests (ROI) of the heart and the mediastinum on

the anterior planar images. They manually adjusted a circular ROI to the heart and set a rectangular ROI in the upper mediastinum. The heart-to-mediastinum (HM) ratio was calculated for each rater by dividing the mean counts per pixel in the cardiac ROI by the mean counts per pixel in the mediastinal ROI. Finally, mean HM ratios of all three raters were calculated. To validate the diagnostic accuracy of MIBG scintigraphy in our data, we used a cut-off value of 2.76 for delayed HM ratio, which was based on a meta-analysis (Orimo et al., 2012), and converted to a camera setting with medium-energy collimators (Brumberg et al., 2019).

2.7. Statistical analysis

Statistical analysis was performed with the commercial software package JMP software version 14.0 (SAS Institute Inc., Car, North CA). Sample size calculation was based on the primary hypothesis that the relative number of p-alpha-syn-positive structures in skin biopsy correlates with HM ratio, and revealed a necessary sample of 45 patients. Numerical data were tested for normal distribution using the Shapiro-Wilk test. Group comparison between PD and MSA and exploratory post hoc group comparison between p-syn-positive and -negative subjects were performed with two-sided Fisher's exact test, student's *t*-test, and Mann-Whitney *U* test as appropriate. Correlations between skin biopsy, imaging, and clinical variables were analyzed with a multivariate analysis and Spearman's ρ over all patients. 2-way full factorial analysis of variance was used to test the effect of diagnosis and p-alpha-syn deposits in autonomic skin structures on HM ratio. Last, we calculated sensitivity and specificity for the diagnostic criteria (i) p-alpha-syn-positivity in autonomic structures, (ii) p-alpha-syn-negativity in somatosensory fibers, and (iii) reduced HM ratio with PD as positive and MSA as negative condition. For all analyses, we considered p values $<$ 0.05 as significant.

2.8. Ethics and protocol approval

The study was approved by the Institutional Review Board of the Julius-Maximilian-University, Würzburg, Germany, and by the Governmental Radiation Protection Authority (Bundesamt für Strahlenschutz, Salzgitter, Germany, Aktenzeichen: Z5–22463/2–2017-006). The study was conducted according to ethical standards in line with the Helsinki Declaration of 1975 (and as revised in 1983). All patients gave written informed consent to participate.

3. Results

3.1. Patients

Four subjects were excluded because of a final diagnosis of progressive supranuclear palsy (two patients) or the diagnosis of comorbidities within 12 months after MIBG scintigraphy (congestive heart failure and peripheral neuropathy, respectively). The remaining 42 patients had a diagnosis of PD or MSA (21 patients (nine women/12 men) in each group). Of the MSA patients, 15 (seven females/eight males) had a diagnosis of MSA with predominant parkinsonism (MSA-P) and six (two females/four males) had MSA with predominant cerebellar ataxia (MSA-C). Gender, age, and disease duration at biopsy did not significantly differ between PD and MSA patients. Patients with MSA had a more rapid disease progression ($p = 0.001$), a higher Unified Parkinson's Disease Rating Scale part III score in the medication "on" state ($p <$ 0.001), and a higher score on the non-motor symptom scale ($p = 0.04$) than patients with PD (Table 1).

3.2. Dermal p-alpha-syn deposition in PD and MSA

P-alpha-syn deposits were observed in dermal nerve fibers of ten patients with PD (47.6%) and 17 patients with MSA (81.0%; MSA-P: 13 patients, MSA-C: four patients). In PD, p-alpha-syn-positive dermal nerve fibers most often innervated autonomic structures such as blood vessels, erector pilorum muscles, or sweat glands (six patients, 28.6%). In two patients (9.5%), p-alpha-syn deposits were found in somatosensory fibers of the subepidermal plexus, and two patients (9.5%) had positive fibers within dermal nerve bundles not attached to a certain structure. Patients with MSA predominantly had p-alpha-syn deposits in somatosensory fibers (eight patients, 38.1%; MSA-P: six patients, MSA-C: two patients), followed by deposits in dermal nerve bundles (five patients, 23.8%; MSA-P: three patients, MSA-C: two patients). Two patients (9.5%, both with MSA-P) showed p-alpha-syn-positivity in autonomic and somatosensory fibers, and in two cases (9.5%, both with MSA-P), deposits were observed in autonomic fibers only. In eight PD patients with p-alpha-syn-positive fibers (80.0%) and in four of p-syn-positive MSA patients (23.5%), deposits were detected in anti-TH-immunoreactive fibers. Anti-VIP- and p-syn-positive fibers were detected in five of p-syn-positive PD patients (50.0%) and in one MSA patient (5.9%). The percentage for different types of p-syn-positive autonomic structures in relation to total positive autonomic structures was similar in PD (skin vessels: 40%, erector pilorum muscles: 40%, sweat glands: 20%) and MSA (64%, 9%, 27%). P-alpha-syn pathology tended to be more frequent ($p = 0.05$) and was more often located in somatosensory fibers ($p = 0.01$) in MSA compared with PD. No significant differences were found between PD and MSA regarding the involvement of autonomic fibers ($p = 0.72$) (Table 1). Cases with PD had more often p-alpha-syn-positive anti-TH-immunoreactive adrenergic fibers ($p = 0.01$) and anti-VIP-immunoreactive cholinergic fibers ($p = 0.02$) when compared to MSA. In p-alpha-syn-positive subjects, the median number of deposits (PD: 5 (range 1–16); MSA: 5 (1–37); $p = 0.63$) and the median percentage of positive biopsy sites (PD: 25% (25–67%); MSA: 50% (25–100%); $p = 0.06$) did not differ between groups. P-alpha-syn-positivity in autonomic structures yielded a sensitivity of 28.6% and a

Table 1
Demographic and clinical variables of patients with PD and MSA.

	PD	MSA	*p* value
Gender (females/males)	9/12	9/12	1.000*
Age at onset (median (range))	58 (25–73)	61.5 (43–73)	0.343#
Age at biopsy [years] (mean ± SD)	63.3 ± 11.6	64.1 ± 9.0	0.790°
Disease duration at biopsy (median (range))	5 (1−21)	3 (1−12)	0.062#
Disease progression (median (range))	2.5 (0.3–6)	1 (0.25–3.3)	0.001#
UPDRS total (mean ± SD)	57.0 ± 26.7	91.3 ± 49.5	0.296°
UPDRS III on (mean ± SD)	26.6 ± 13.1	47.8 ± 10.9	<0.001°
UPDRS III off (mean ± SD)	38.0 ± 16.2	45.5 ± 12.2	0.363°
NMS (mean ± SD)	40.3 ± 25.0	98.3 ± 52.4	0.042°
p-alpha-syn deposits [number of patients] (%)	10 (47.6)	17 (81.0)	0.052*
p-alpha-syn deposits in autonomic structures [number of patients] (%)	6 (28.6)	4 (19.0)	0.719*
p-alpha-syn deposits in somatosensory fibers [number of patients] (%)	2 (9.5)	10 (43.5)	0.015*
p-alpha-syn deposits in dermal nerve bundles [number of patients] (%)	2 (9.5)	5 (23.8)	0.410*
IENFD distal leg [fibers/mm] (median (range))	2.9 (0.0–9.4)	4.6 (1.3–11.3)	0.233#
IENFD proximal leg [fibers/mm] (median (range))	5.1 (3.2–11.7)	9.1 (2.0–15.2)	0.034#
IENFD back [fibers/mm] (median (range))	8.7 (2.2–26.9)	13.8 (3.5–37.9)	0.101#
IENFD neck [fibers/mm] (median (range))	9.0 (2.2–18.3)	9.0 (2.9–15.3)	0.620#
HM ratio (mean ± SD)	1.94 ± 0.63	2.91 ± 0.96	<0.001°

p values are displayed for group comparison by using Fisher's exact*, Mann-Whitney $U^{\#}$ and student's t° test. Abbreviations: HM, heart-to-mediastinum ratio; IENFD, intraepidermal nerve fiber density; MSA, multiple system atrophy; NMS, non-motor symptom scale; p-alpha-syn, phosphorylated alpha-synuclein; PD, idiopathic Parkinson's disease; SD, standard deviation; UPDRS, Unified Parkinson's Disease Rating Scale.

specificity of 81.0%, and negative findings for p-alpha-syn in somatosensory fibers showed a sensitivity of 90.5% and a specificity of 47.6% to separate patients with PD from patients with MSA.

3.3. Quantification of epidermal and dermal autonomic nerve fibers

Eight patients had a reduced SNAP or nerve conduction velocity and were therefore excluded from this analysis. Quantification of small intraepidermal nerve fibers showed a lower median IENFD in biopsies of the thigh in PD compared to MSA patients ($p = 0.03$) (Table1). The difference was also significant after correction for gender and age (ANCOVA: $p = 0.02$). The IENFD of the distal leg (ANCOVA: $p = 0.15$), back (ANCOVA: $p = 0.12$) and neck (ANCOVA: $p = 0.60$) did not differ between groups but tended to be lower in PD compared to MSA. No significant differences between groups were found in terms of erector pili and sweat gland innervation, or noradrenergic and cholinergic sudomotor innervation. Over all patients, IENFD of the distal leg was positively correlated with disease duration ($\rho = 0.37$, $p = 0.05$), which was not significant after correction for age ($p = 0.07$).

3.4. Cardiac MIBG scintigraphy differentiates between PD and MSA

Cardiac MIBG scintigraphy revealed a lower mean HM ratio in PD compared to MSA patients ($p < 0.001$) (Table 1 and Fig. 1). Applying a cut-off value of 2.76, 19 of 21 patients with PD and 14 of 21 subjects with MSA were concordant with their clinical diagnosis, resulting in a sensitivity of 90.5% and a specificity of 66.6% in the study sample.

3.5. Association of cardiac and dermal autonomic involvement

Mean HM ratio of patients with p-alpha-syn deposits in autonomic structures was significantly lower than of those patients without p-alpha-syn-positive autonomic fibers (1.42 ± 0.51 vs. 2.74 ± 0.83; $p < 0.0001$) (Fig. 1). A reduced HM ratio in patients with proven p-alpha-syn pathology in somatosensory fibers (with vs. without: 2.83 ± 1.08 vs. 2.26 ± 0.86; $p = 0.12$) or in dermal nerve bundles only (with vs. without: 2.38 ± 0.97 vs. 2.68 ± 0.90; $p = 0.45$) was not observed. Of note, this was also the case when comparing these groups with p-alpha-syn-negative patients only. Multivariate analysis in all patients did not show a significant correlation of HM ratio with any other variable, particularly not with the absolute or relative number of p-alpha-syn-positive structures, the percentage of p-alpha-syn-positive skin biopsy sites, or any other marker of dermal innervation. 2-way factorial ANOVA revealed that diagnosis (PD vs. MSA; $p = 0.007$) and p-alpha-syn pathology in autonomic skin elements ($p < 0.0001$) had an effect with regards to the HM ratio but did not have an interaction, indicating that the involvement of autonomic structures in skin biopsy had no different effect in either patient group.

3.6. Dermal p-alpha-syn deposition, MIBG scintigraphy, and diagnostic categories of different strength

Thirty patients had a typical clinical presentation (16 tPD, 14 tMSA), whereas 12 patients (five PD, seven MSA) had ambiguous clinical features and were referred to the PD/MSA overlap group. None of the patients with tPD had p-alpha-syn deposits in somatosensory fibers, and none of the patients with tMSA had p-alpha-syn-positive autonomic structures, revealing a negative predictive value of 100% for these patient groups. The two patients who had p-alpha-syn in both fiber types belonged to the PD/MSA overlap group. The mean MIBG HM ratio was lower in the PD and PD/MSA overlap groups compared to MSA patients ($p < 0.001$). Concordant results were found in 16 patients (i.e., pathological HM ratio and p-alpha-syn in autonomic fibers [four tPD, three PD/MSA overlap], normal HM ratio with p-alpha-syn in somatosensory fibers [five tMSA, two PD/MSA overlap], or pathological HM ratio and p-alpha-syn in both fiber types [two PD/MSA overlap) (Fig. 2), discordant findings in only four patients (one PD/MSA overlap with normal HM ratio and p-alpha-syn in autonomic fibers, one PD/MSA overlap with pathological HM ratio and p-alpha-syn in somatosensory fibers, two tMSA with pathological HM ratio and p-alpha-syn in somatosensory fibers) (Table 2).

4. Discussion

We aimed to investigate the association of dermal p-alpha-syn depositions and cardiac denervation in patients with PD and MSA. Our main finding is that p-alpha-syn depositions in peripheral autonomic nerve fibers are associated with sympathetic cardiac denervation, whereas p-alpha-syn pathology in somatosensory fibers or dermal nerve bundles was not related to decreased cardiac innervation. Accordingly,

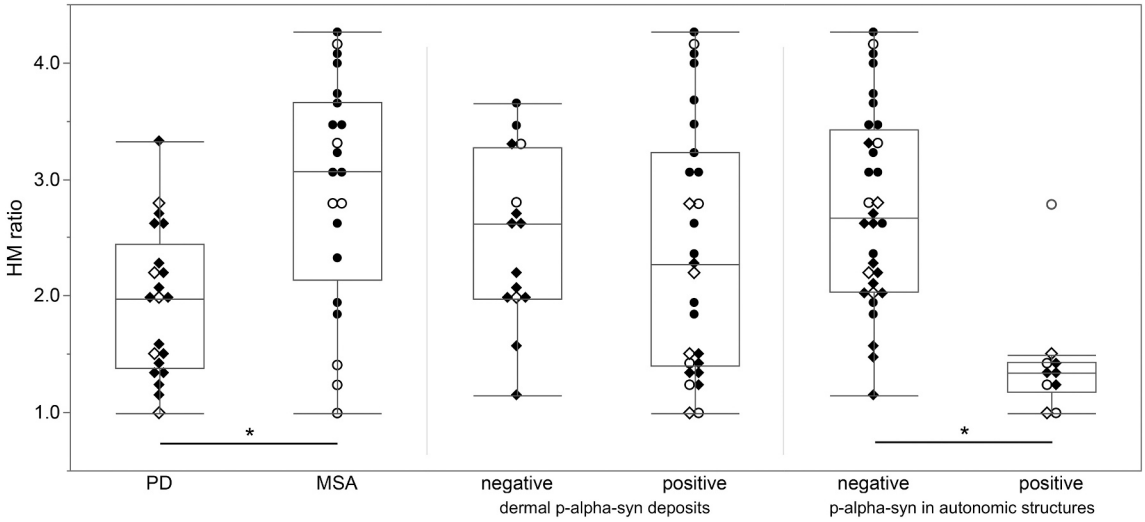

Fig. 1. Boxplots of delayed heart-to-mediastinum (HM) ratio of MIBG scintigraphy.
Left panel shows the comparison of patients with Parkinson's disease (PD) and multiple system atrophy (MSA). The middle shows patients without vs. with proof of phosphorylated alpha-synuclein (p-alpha-syn) depositions in dermal nerve fibers. On the right side, patients, who were negative for p-alpha-syn in autonomic skin elements are compared with positive patients. Patients with PD are represented by squares, circles display patients with MSA. Open squares and open circles indicate patients with overlapping clinical symptoms (PD/MSA overlap). * $p < 0.0001$, two-sample *t*-test. Abbreviations: MIBG = [^{123}I]-metaiodobenzylguanidine.

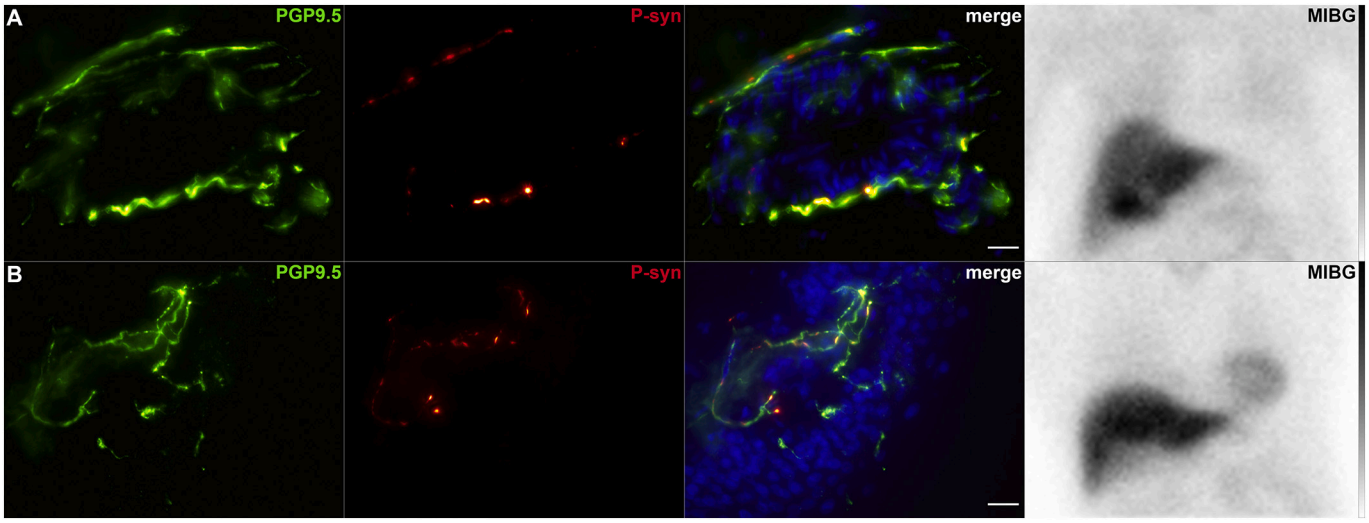

Fig. 2. Photomicrographs of double-immunofluorescence staining with anti-p-syn (red) and anti-PGP9.5 (green), and MIBG scintigraphy.
P-alpha-syn depositions in autonomic structures, such as blood vessels, were associated with a reduced cardiac HM ratio (A). Patients with deposits in somatosensory fibers of the subepidermal plexus predominantly showed a normal cardiac innervation (B). Cell nuclei are stained with DAPI (blue). Scale bar = 20 μm; gradient bar is scaled to minimal and maximal MIBG uptake. Abbreviations: MIBG = [^{123}I]-metaiodobenzylguanidine.

Table 2
Concordance of skin biopsy findings and MIBG scintigraphy.

	tPD	PD/MSA overlap	tMSA
Gender (females/males)	6 /10	5/7	7/7
p-alpha-syn deposits [number of patients] (%)	6 (37.5)	9 (75.0)	12 (85.7)
p-alpha-syn deposits in autonomic structures [number of patients] (%)	4 (25.0)	6 (50.0)	0 (0.0)
p-alpha-syn deposits in somatosensory fibers [number of patients] (%)	0 (0.0)	5 (41.7)	7 (50.0)
p-alpha-syn deposits in dermal nerve bundles [number of patients] (%)	2 (12.5)	0 (0.0)	5 (35.7)
HM ratio (mean ± SD)	1.96 ± 0.64	2.17 ± 1.00	3.18 ± 0.76
Pathological HM ratio [number of patients] (%)	15 (93.8)	7 (58.3)	4 (28.6)
Normal HM ratio [number of patients] (%)	1 (16.2)	5 (41.7)	10 (71.4)
Concordance MIBG scintigraphy & skin biopsy [number of patients] (%)	4 (100.0 [a])	7 (77.8 [a])	5 (71.4 [a])
Discordance MIBG scintigraphy & skin biopsy [number of patients] (%)	0 (0.0 [a])	2 (22.2 [a])	2 (28.6 [a])

[a] Denominator refers to number of patients with p-alpha-sun deposits in autonomic and/or somatosensory fibers. Abbreviations: HM, heart-to-mediastinum; MIBG, [^{123}I]-metaiodobenzylguanidine; p-alpha-syn, phosphorylated alpha-synuclein; PD/MSA overlap, PD and MSA patients with overlapping symptoms; SD, standard deviation; tMSA, multiple system atrophy with typical clinical presentation; tPD, Parkinson's disease with typical clinical presentation.

p-alpha-syn deposition in autonomic fibers and cardiac sympathetic denervation in MIBG scintigraphy were mainly found in PD, while p-alpha-syn deposition in somatosensory fibers and preserved cardiac sympathetic innervation were mostly in MSA. However, discordant findings could be found in some patients and were associated with clinical overlapping/discordant features in PD and MSA.

The coincidence of autonomic alpha-synuclein pathology in the skin and cardiac denervation suggests that alpha-synuclein affects cardiac sympathetic neurons and contributes to neuronal cell loss in these patients. In fact, prior studies identified alpha-synuclein-positive neurites and Lewy bodies in neurons within the heart of patients with PD (Iwanaga et al., 1999; Okada et al., 2004), possibly causing degeneration of cardiac sympathetic nerves early in the disease course (Orimo et al., 2008). Our data demonstrate that autonomic denervation and p-alpha-syn deposition is associated with the clinical picture of idiopathic PD, supporting the diagnostic value of both methods. However, in contrast to some recent studies (Donadio et al., 2014; Donadio et al., 2017), we did not find a reduction in sweat gland or erector pilorum muscle innervation associated with p-alpha-syn deposition in autonomic nerve fibers. We therefore cannot give a conclusion on the effect of p-alpha-syn deposits on dermal sympathetic denervation. A reason could be that p-alpha-syn was mostly found in vasomotor fibers rather than sudomotor or pilomotor fibers, and sweat gland and erector pilorum muscle innervation may therefore not be significantly affected in our cohort.

The sensitivity (90.5%) of MIBG scintigraphy for PD in this study was expectedly high, whereas specificity (66.6%) was slightly lower but within the 95% confidence interval (CI) of a recent meta-analysis (sensitivity: 90.2% (CI 84.4–93.9%); specificity: 81.9% (CI 56.1–94.1%)) (Orimo et al., 2012). Likewise, fiber-type involvement differed between PD and MSA but was not 100% specific for both groups as previously reported (Doppler et al., 2015). However, sensitivity and specificity to separate PD from MSA by using either p-alpha-syn deposits in autonomic structures (28.6% and 81.0%) or negativity for p-alpha-syn in somatosensory fibers (90.5% and 47.6%) as diagnostic criteria are below published values. Recent studies reported 92.3% specificity for autonomic p-alpha-syn deposits (Giannoccaro et al., 2020) and 72.0% specificity for p-alpha-syn-negativity in somatosensory fibers (Donadio et al., 2020) (note that this reference defined MSA as positive condition and evaluated the diagnostic criterion "p-alpha-syn-positivity in somatosensory fibers" why the values for sensitivity and specificity were adjusted to meet the present definition of positive [PD] and negative cases [MSA]). The discrepancies might be related to the selection of included patients, since the reported values of 97.5–100.0% sensitivity and 100.0% specificity for MIBG scintigraphy (Donadio et al., 2020; Giannoccaro et al., 2020) do not reflect clinical reality and exceed the diagnostic accuracy of this method (Orimo et al., 2012). In our study, the clinical diagnosis was blinded to the results of MIBG scintigraphy and relied on clinical guideline criteria only (Gilman et al., 2008; Postuma et al., 2015) preventing the identification of patients with inconclusive pathology of the peripheral nervous system before study inclusion, and thus a possible selection bias. Of relevance, specificity of both methods was much higher in our study when patients with overlapping features were excluded, suggesting that these patients must be considered separately from patients with typical clinical presentation. Involvement of autonomic or somatosensory nerve fibers in p-alpha-syn deposition,

however, may contribute to the differential diagnosis in patients with overlapping features and may be combined with neuroimaging to increase the diagnostic confidence. Seven patients with concordant findings belonged to the PD/MSA overlap group, suggesting that the combination of skin biopsy and MIBG scintigraphy can improve diagnostic confidence in these patients.

Four patients showed inconclusive findings, of which two were assigned to the PD/MSA overlap group. Remarkably, two more patients in this group had the combination of p-alpha-syn deposition in autonomic and somatosensory fibers. This indicates that mechanisms of both peripheral autonomic degeneration and somatosensory involvement may occur to some extent in both diseases or in a clinically indefinite patient cluster, supporting the idea of the existence of overlapping syndromes. The latter has been suggested before, based on overlapping clinical features (Krismer et al., 2014), potential impairment of cardiac innervation in both diseases (Nagayama et al., 2010), and histopathological findings (i.e., alpha-synuclein-related pathology in thoracic sympathetic ganglia in patients with advanced MSA) (Sone et al., 2005). Either peripheral autonomic degeneration or somatosensory involvement in the majority of patients, and coincidence of autonomic and somatosensory involvement in single patients, supports the concept that deposition of p-alpha-syn in specific cell types may be facilitated by a selective cell or neuronal vulnerability related to the genetic profile of patients (Walsh and Selkoe, 2016). We speculate that such a profile might determinate peripheral nervous system involvement, and its expression is more frequent in either PD or MSA but does not represent an exclusive feature for the respective entity. Remarkably, the HM ratio was lower in PD patients with than without dermal p-alpha-syn deposition, suggesting different extents of affection of autonomic nerves within the PD group.

Two PD patients and five patients with MSA had p-alpha-syn deposits in dermal nerve bundles, which may include both autonomic and somatosensory fibers. We reviewed their anti-TH- and anti-VIP-immunoreactivity to clarify if these fibers might be autonomic: p-alpha-syn-positive fibers of one PD patient (with pathologic HM ratio) were also anti-TH-positive, whereas p-alpha-syn deposits of all other subjects were negative for both autonomic markers. This observation is in line with the overall results of the study, however, we did not consider anti-TH-positivity as confirmatory for autonomic involvement in this case, since preclinical evidence indicates that some sensory fibers of the skin may show anti-TH-immunoreactivity (Brumovsky et al., 2006) – and vice-versa, the lack of anti-TH- and anti-VIP-positivity does not prove that these fibers are actual somatosensory.

The overall detection rate of dermal p-alpha-syn depositions match previous findings, although detection of p-alpha-syn in 47.6% of PD patients in our study was below the reported range of 51.6–100% (Donadio et al., 2014; Donadio et al., 2018a; Doppler et al., 2014; Doppler et al., 2017; Zange et al., 2015). One possible explanation for the low rate could be that we did not exclude subjects with early disease onset, who have more likely PD gene mutations (Blauwendraat et al., 2020), while the presence of dermal p-alpha-syn deposits in different forms of monogenic PD is still subject to current research (Doppler et al., 2018). Out of three patients with early onset PD, two were tested negative for PRKN and LRRK2 mutations (one with p-alpha-syn in somatosensory fibers, one without p-alpha-syn deposits), whereas no genetic testing was performed in the remaining patient (p-alpha-syn-negative). Although compound heterozygosity for the PRKN gene causes up to 50.0% of early onset PD (Jankovic and Tan, 2020), other mutations related to early onset PD, and thus, a possible effect on positivity rate cannot be excluded. The percentage of MSA patients with dermal p-alpha-syn pathology in our sample (81.0%) was slightly higher than previously observed (66.6%) (Donadio et al., 2018b; Doppler et al., 2015), mainly driven by the high detection rate in patients with MSA-P. As could be assumed from the clinical profile, no subjects with MSA and predominant cerebellar ataxia had p-alpha-syn deposits in autonomic skin elements, but 33.3% had deposits in somatosensory fibers; this indicates the involvement of the peripheral nervous system in both MSA subtypes, with more clinical as well as histopathological similarities between MSA-P and PD. However, due to the small sample size, final conclusions cannot be drawn on this subgroup.

This study has several limitations. First, the sensitivity of skin biopsy is limited, most probably because p-alpha-syn-positive fibers are rare and do not occur in all skin sections. Second, reduced cardiac MIBG uptake can be related to alpha-synuclein aggregation (Iwanaga et al., 1999; Okada et al., 2004; Orimo et al., 2008), but is an unspecific measure that does not prove Lewy body disease and particularly not alpha-synuclein pathology. It may also be caused by (occult) congestive heart failure, ischemic heart disease, or neuropathy (Henzlova et al., 2016; Jacobson et al., 2010). This was the case in two subjects with MSA in our study sample, who therefore had to be excluded. Third, the clinical diagnosis as reference standard is limited in parkinsonian syndromes, since it is not confirmed by autoptic findings in up to 20% of patients (Hughes et al., 2002; Litvan et al., 1997). Future studies on this topic with histopathological post-mortem confirmation are therefore warranted.

5. Conclusions

This study provides evidence that alpha-synuclein engages peripheral neurodegeneration and mediates the impairment of cardiac sympathetic neurons in patients with synucleinopathies. Furthermore, it indicates that PD and MSA share pathophysiologic mechanisms of peripheral nervous system dysfunction with a clinical and peripheral histopathological overlap.

Funding

This study was sponsored by the Interdisziplinäres Zentrum für klinische Forschung (IZKF) of the University Hospital Würzburg. Joachim Brumberg (grant number Z-2/74) and Anastasia Kuzkina received a scholarship from the IZKF of the University Hospital Würzburg. Joachim Brumberg received a scholarship from the German Research Foundation (Deutsche Forschungsgemeinschaft, DFG, grant number BR 6121/1-1). This publication was supported by the Open Access Publication Fund of the University of Würzburg.

Declaration of Competing Interest

None.

References

Blauwendraat, C., et al., 2020. The genetic architecture of Parkinson's disease. Lancet Neurol. 19, 170–178.
Bombardieri, E., et al., 2010. 131I/123I-metaiodobenzylguanidine (mIBG) scintigraphy: procedure guidelines for tumour imaging. Eur. J. Nucl. Med. Mol. Imaging 37, 2436–2446.
Borghammer, P., 2018. How does parkinson's disease begin? Perspectives on neuroanatomical pathways, prions, and histology. Mov. Disord. 33, 48–57.
Brumberg, J., et al., 2019. Imaging cardiac sympathetic innervation with MIBG: linear conversion of the heart-to-mediastinum ratio between different collimators. EJNMMI Phys. 6, 12.
Brumovsky, P., et al., 2006. Tyrosine hydroxylase is expressed in a subpopulation of small dorsal root ganglion neurons in the adult mouse. Exp. Neurol. 200, 153–165.
Burre, J., et al., 2018. Cell biology and pathophysiology of alpha-synuclein. Cold Spring Harb. Perspect. Med. 8.
Dickson, D.W., et al., 1999. Widespread alterations of α-synuclein in multiple system atrophy. Am. J. Pathol. 155, 1241–1251.
Dickson, D.W., et al., 2009. Neuropathological assessment of Parkinson's disease: refining the diagnostic criteria. Lancet Neurol. 8, 1150–1157.
Donadio, V., et al., 2014. Skin nerve alpha-synuclein deposits: a biomarker for idiopathic Parkinson disease. Neurology. 82, 1362–1369.
Donadio, V., et al., 2017. A new potential biomarker for dementia with Lewy bodies: skin nerve alpha-synuclein deposits. Neurology. 89, 318–326.
Donadio, V., et al., 2018a. Skin nerve phosphorylated alpha-synuclein deposits in Parkinson disease with orthostatic hypotension. J. Neuropathol. Exp. Neurol. 77, 942–949.

Donadio, V., et al., 2018b. Skin alpha-synuclein deposits differ in clinical variants of synucleinopathy: an in vivo study. Sci. Rep. 8, 14246.
Donadio, V., et al., 2020. Skin biopsy may help to distinguish multiple system atrophy-Parkinsonism from Parkinson's disease with orthostatic hypotension. Mov. Disord. 35, 1649–1657.
Doppler, K., et al., 2014. Cutaneous neuropathy in Parkinson's disease: a window into brain pathology. Acta Neuropathol. 128, 99–109.
Doppler, K., et al., 2015. Distinctive distribution of phospho-alpha-synuclein in dermal nerves in multiple system atrophy. Mov. Disord. 30, 1688–1692.
Doppler, K., et al., 2017. Dermal phospho-alpha-synuclein deposits confirm REM sleep behaviour disorder as prodromal Parkinson's disease. Acta Neuropathol. 133, 535–545.
Doppler, K., et al., 2018. Dermal phospho-alpha-synuclein deposition in patients with Parkinson's disease and mutation of the glucocerebrosidase gene. Front. Neurol. 9, 1094.
Flotats, A., et al., 2010. Proposal for standardization of 123I-metaiodobenzylguanidine (MIBG) cardiac sympathetic imaging by the EANM Cardiovascular Committee and the European Council of Nuclear Cardiology. Eur. J. Nucl. Med. Mol. Imaging 37, 1802–1812.
Giannoccaro, M.P., et al., 2020. Comparison of 123I-MIBG scintigraphy and phosphorylated alpha-synuclein skin deposits in synucleinopathies. Parkinsonism Relat. Disord. 81, 48–53.
Gilman, S., et al., 2008. Second consensus statement on the diagnosis of multiple system atrophy. Neurology. 71, 670–676.
Henzlova, M.J., et al., 2016. ASNC imaging guidelines for SPECT nuclear cardiology procedures: stress, protocols, and tracers. J. Nucl. Cardiol. 23, 606–639.
Hughes, A.J., et al., 2002. The accuracy of diagnosis of parkinsonian syndromes in a specialist movement disorder service. Brain. 125, 861–870.
Iwanaga, K., et al., 1999. Lewy body-type degeneration in cardiac plexus in Parkinson's and incidental Lewy body diseases. Neurology. 52, 1269–1271.
Jacobson, A.F., et al., 2010. Myocardial iodine-123 meta-iodobenzylguanidine imaging and cardiac events in heart failure. Results of the prospective ADMIRE-HF (AdreView Myocardial Imaging for Risk Evaluation in Heart Failure) study. J. Am. Coll. Cardiol. 55, 2212–2221.
Jankovic, J., Tan, E.K., 2020. Parkinson's disease: etiopathogenesis and treatment. J. Neurol. Neurosurg. Psychiatry 91, 795–808.
Kimura, J., 2013. Electrodiagnosis in Diseases of Nerve and Muscle: Principles and Practice. Oxford University Press, New York.
Krismer, F., et al., 2014. Multiple system atrophy as emerging template for accelerated drug discovery in alpha-synucleinopathies. Parkinsonism Relat. Disord. 20, 793–799.
Krismer, F., et al., 2019. Morphometric MRI profiles of multiple system atrophy variants and implications for differential diagnosis. Mov. Disord. 34, 1041–1048.
Lauria, G., et al., 2005. EFNS guidelines on the use of skin biopsy in the diagnosis of peripheral neuropathy. Eur. J. Neurol. 12, 747–758.
Lebouvier, T., et al., 2010. Colonic biopsies to assess the neuropathology of Parkinson's disease and its relationship with symptoms. PLoS One 5, e12728.
Litvan, I., et al., 1997. What is the accuracy of the clinical diagnosis of multiple system atrophy? A clinicopathologic study. Arch. Neurol. 54, 937–944.
Meyer, P.T., et al., 2017. (18)F-FDG PET in Parkinsonism: differential diagnosis and evaluation of cognitive impairment. J. Nucl. Med. 58, 1888–1898.
Nagayama, H., et al., 2010. Abnormal cardiac [(123)I]-meta-iodobenzylguanidine uptake in multiple system atrophy. Mov. Disord. 25, 1744–1747.
Okada, Y., et al., 2004. Lewy bodies in the sinoatrial nodal ganglion: clinicopathological studies. Pathol. Int. 54, 682–687.
Orimo, S., et al., 1999. (123)I-metaiodobenzylguanidine myocardial scintigraphy in Parkinson's disease. J. Neurol. Neurosurg. Psychiatry 67, 189–194.
Orimo, S., et al., 2008. Axonal alpha-synuclein aggregates herald centripetal degeneration of cardiac sympathetic nerve in Parkinson's disease. Brain. 131, 642–650.
Orimo, S., et al., 2012. 123I-MIBG myocardial scintigraphy for differentiating Parkinson's disease from other neurodegenerative parkinsonism: a systematic review and meta-analysis. Parkinsonism Relat. Disord. 18, 494–500.
Postuma, R.B., et al., 2015. MDS clinical diagnostic criteria for Parkinson's disease. Mov. Disord. 30, 1591–1601.
Rocha, E.M., et al., 2018. Alpha-synuclein: pathology, mitochondrial dysfunction and neuroinflammation in Parkinson's disease. Neurobiol. Dis. 109, 249–257.
Schneider, C.A., et al., 2012. NIH Image to ImageJ: 25 years of image analysis. Nat. Methods 9, 671–675.
Sone, M., et al., 2005. alpha-Synuclein-immunoreactive structure formation is enhanced in sympathetic ganglia of patients with multiple system atrophy. Acta Neuropathol. 110, 19–26.
Spillantini, M.G., 1999. Parkinson's disease, dementia with Lewy bodies and multiple system atrophy are alpha-synucleinopathies. Parkinsonism Relat. Disord. 5, 157–162.
Treglia, G., et al., 2012. MIBG scintigraphy in differential diagnosis of Parkinsonism: a meta-analysis. Clin. Auton. Res. 22, 43–55.
Vilas, D., et al., 2016. Assessment of α-synuclein in submandibular glands of patients with idiopathic rapid-eye-movement sleep behaviour disorder: a case-control study. Lancet Neurol. 15, 708–718.
Walsh, D.M., Selkoe, D.J., 2016. A critical appraisal of the pathogenic protein spread hypothesis of neurodegeneration. Nat. Rev. Neurosci. 17, 251–260.
Zange, L., et al., 2015. Phosphorylated alpha-synuclein in skin nerve fibres differentiates Parkinson's disease from multiple system atrophy. Brain. 138, 2310–2321.